communications materials

PERSPECTIVE

https://doi.org/10.1038/s43246-023-00341-y OPEN

Functional two-dimensional high-entropy materials

Srinivasa Kartik Nemani[1,6], Mohammad Torkamanzadeh[2,3,6], Brian C. Wyatt[1,6], Volker Presser[2,3,4]✉ & Babak Anasori[1,5]✉

Multiple principal element or high-entropy materials have recently been studied in the two-dimensional (2D) materials phase space. These promising classes of materials combine the unique behavior of solid-solution and entropy-stabilized systems with high aspect ratios and atomically thin characteristics of 2D materials. The current experimental space of these materials includes 2D transition metal oxides, carbides/carbonitrides/nitrides (MXenes), dichalcogenides, and hydrotalcites. However, high-entropy 2D materials have the potential to expand into other types, such as 2D metal-organic frameworks, 2D transition metal carbo-chalcogenides, and 2D transition metal borides (MBenes). Here, we discuss the entropy stabilization from bulk to 2D systems, the effects of disordered multi-valent elements on lattice distortion and local electronic structures and elucidate how these local changes influence the catalytic and electrochemical behavior of these 2D high-entropy materials. We also provide a perspective on 2D high-entropy materials research and its challenges and discuss the importance of this emerging field of nanomaterials in designing tunable compositions with unique electronic structures for energy, catalytic, electronic, and structural applications.

Historically, alloying has been a popular method in metallurgy to derive unique and superior properties in metals[1,2]. Efforts toward the exploration of alloys with multiple principal metals at equimolar or near equimolar ratios have led to the realization of multicomponent systems with unique structure–property synergies[3,4]. These materials are stabilized by the increased effect of configurational entropy, as demonstrated in the high-entropy alloys phase space at the bulk scale since the 2000s[5–9].

Furthermore, the inclusion of non-metallic species, such as carbon, hydrogen, nitrogen, and oxygen, has been studied either at a few at.% in high-entropy alloys or to occupy the interstitial sites of the metal lattice to form new compounds to accentuate the properties of these materials. For example, the addition of 2 at.% oxygen increases the mechanical strength and ductility[10], <0.5 at.% carbon enhances phase stability and wear resistance[11,12], <0.6 at.% boron improves hardness, while the inclusion of hydrogen at ~50 mass% ppm reduces the stacking fault energies leading to localized strain hardening in alloys[13]. Consequently, the high-entropy materials space has expanded further into non-metallic compounds with bulk nitride films[14,15], crystalline[16–18] and amorphous[19] oxides, carbides[20,21], borides[22], silicides[23,24], and chalcogenides[25] mostly since 2015. This expansion has been driven by their potential for attractive properties in applications ranging from mechanical[20], catalysis[26,27], thermal[28,29], electrical, energy storage, and harvesting[30]. Some of the compounds reported to date have a low or medium entropic

[1] Department of Mechanical and Energy Engineering, and Integrated Nanosystems Development Institute (INDI), Indiana University, Purdue University, 723W. Michigan Street, West Lafayette, IN 46202, USA. [2] INM—Leibniz Institute for New Materials, Campus D2 2, 66123 Saarbrücken, Germany. [3] Department of Materials Science & Engineering, Saarland University, Campus D2 2, 66123 Saarbrücken, Germany. [4] Saarene—Saarland Center for Energy Materials and Sustainability, Campus C4 2, 66123 Saarbrücken, Germany. [5] School of Materials Engineering, Purdue University, Neil Armstrong Hall of Engineering, 701W Stadium Ave, West Lafayette, IN 47907, USA. [6] These authors contributed equally: Srinivasa Kartik Nemani, Mohammad Torkamanzadeh, Brian C. Wyatt. ✉email: volker.presser@leibniz-inm.de; banasori@iupui.edu

contribution (non-equimolar compositions and less than four principal elements), also referred to as compositionally complex ceramics[31].

The concept of high entropy at the nanoscale was introduced in 2017[32], and further expanded to layered two-dimensional (2D) materials in 2020–2022 with entropy-stabilized multiple principal elements in oxide, chalcogenide, carbide/carbonitride (MXenes), hydroxide forms with promising practical applications[27,33–42]. Furthermore, van der Waals heterostructures of entropy-stabilized 2D chalcogenides and halides have exhibited superconductivity, unique magnetic behavior, and heterogeneous catalytic activity[43]. Figure 1a shows the timeline from the realization of entropy stabilization in bulk phases, alloys in 2004 and ceramics in 2015, to layered 2D materials in 2020–2021. While high-entropy 2D materials are still in their infancy, the combination of their high surface area and functionalities of 2D materials with entropy stabilization brings the promise to accelerate materials discovery for applications such as energy conversion or storage.

In this perspective, we discuss entropy stabilization from bulk to 2D systems, the effects of disordered multi-valent elements on lattice distortion and local electronic structures, and elucidate these changes on the catalytic and electrochemical behavior of 2D high-entropy materials. While in bulk form, these materials have been explored for their stability and mechanical behavior, since no studies have reported the mechanical properties of high-entropy 2D materials, we focus more on applications such as energy conversion and storage, which are current areas of interest for 2D materials.

High entropy structures

The formation and stabilization of high-entropy materials come with various degrees of mixing in the metallic sublattices. Figure 1b shows an array of entropy-stabilized systems where order–disorder transitions are possible with substitutional interfaces (non-equimolar systems)[44], short-range ordering (localized clustering)[45], and complete randomized solid solutions (with an increase in the number of constituents) in a system comprising of multiple elements. Increasing the number of species increases the contribution of the entropy term in Gibbs' free energy equation, making configurational entropy the main contributor to system stability, as shown in Fig. 1c. Unlike in high-entropy alloys, in high-entropy compounds, the presence of non-metals (as we will refer to them as X) in the metal interstitial sites (referred to as M) can lead to complex M–X coordination bonding states[17,46]. Further, the presence of non-metallic sublattices enables a larger selectivity and diversity in the M species with room for elements of larger ionic radii and M–X bond lengths with little effect on

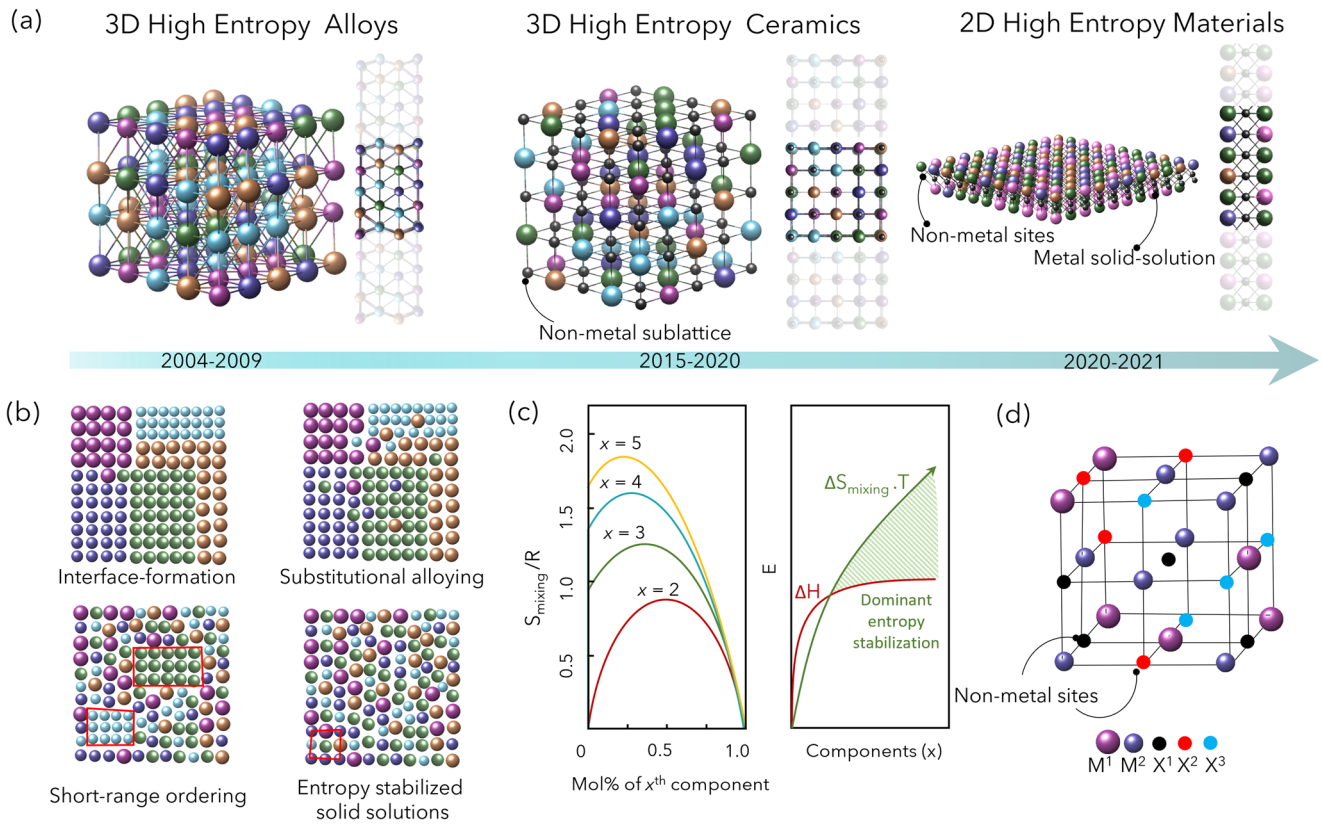

Fig. 1 Progress in high-entropy materials research. a Timeline and progress in entropy-stabilized systems over the past decade with the transition toward high-entropy 2D materials in 2021. **b** Four different degrees of order and disorder between the phase-segregated structures and the ideal entropy-stabilized solid solutions. **b** reproduced with permission from ref. [75] (copyright AAAS, 2021); **c** Configurational entropy change as a function of the number of species (N) and the mole fraction of the Xth component system varying from $N = 2$ to $N = 5$. **c** Reproduced with permission from ref. [17] (copyright Springer Nature, 2015). The maximum entropy is attained at equimolar compositions. Depending on S/R, one distinguishes between low, medium, and high-entropy materials. The panel on the right shows the energy (E) region for dominant entropy effects (shaded area) in a system. Reproduced with permission from ref. [88] (copyright Wiley, 2017). The red line indicates the enthalpic contribution (ΔH), and the line in green shows the entropic contribution (ΔS). **d** A multiple principal element system with 2 metallic and 3 non-metallic species in the crystal lattice as an example of entropy stabilization by both metal and non-metal sites. Entropic contribution from both the sublattices is given by: $\Delta S_{\mathrm{mix}} = -R\left[\left(\sum_{i=1}^{N} x_i \ln x_i\right)_{\mathrm{cation-site}} + \left(\sum_{j=1}^{N} x_j \ln x_j\right)_{\mathrm{anion-site}}\right]$. **d** Reproduced with permission from ref. [49] (copyright, Elsevier, 2020).

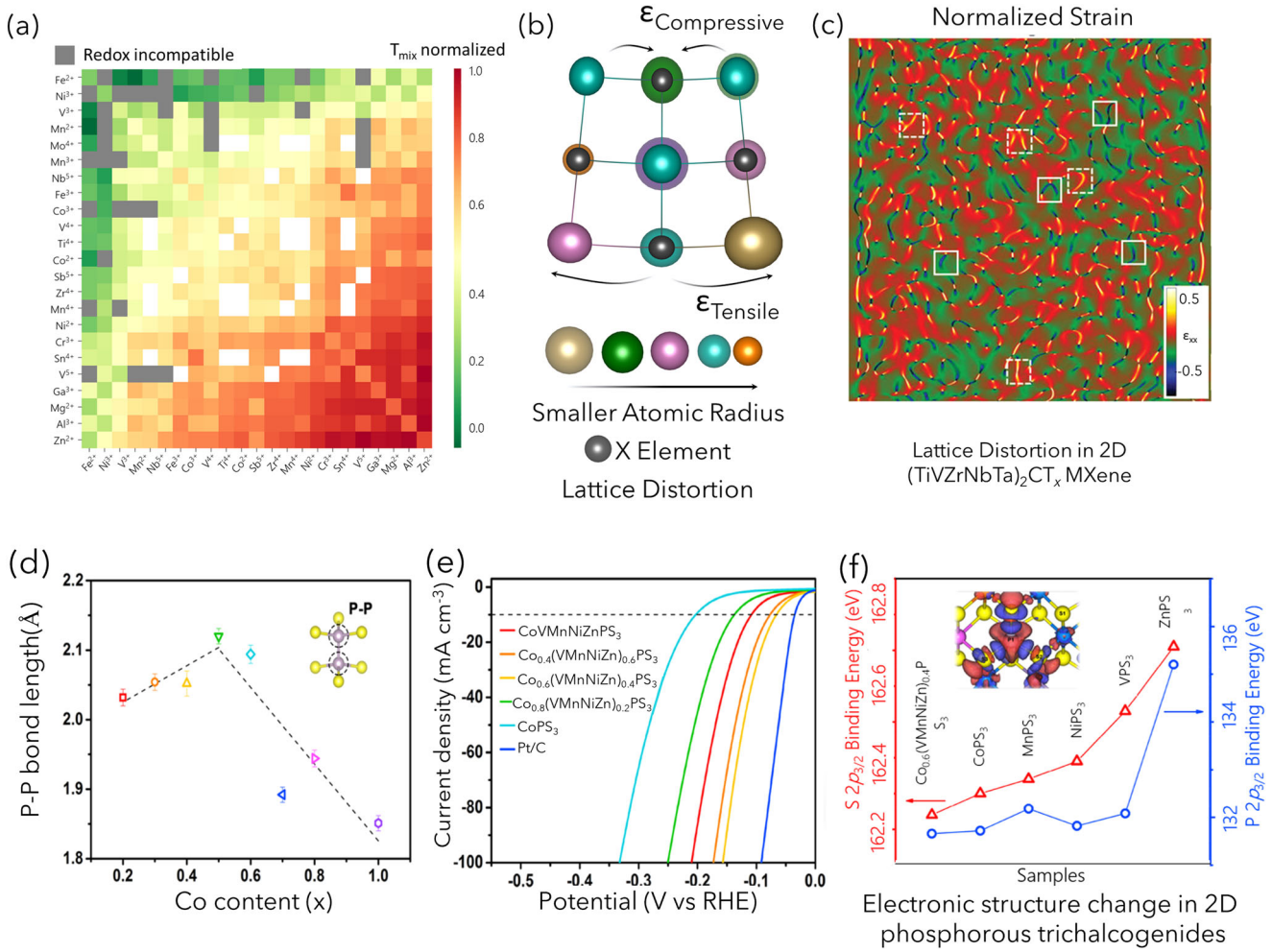

Fig. 2 Compatibility and effect of coordination states in multiple M elements. a Normalized temperature at which two paired cations are stable in a cation-disordered rock-salt structure. **a** reproduced with permission from ref. [56] (copyright Springer Nature, 2021). **b** Mechanical straining of multiple different-sized cations on the distortion of a rock-salt ceramic structure. **c** Mechanical distortion of the lattice of a $(TiVZrNbTa)_2CT_x$ MXene as-measured via scanning transmission electron microscopy (STEM). **c** Reproduced with permission from ref. [38] (copyright Wiley, 2021). **d** Local changes in P–P bond length in a high-entropy $Co_x(VMnNiZn)_{1-x}PS_3$ structure with change in Co[37]. **e** Change in hydrogen evolution reaction behavior based on P–P distance[37]. **f** Binding energy of the S $2p_{3/2}$ and P $2p_{3/2}$ peak as measured via X-ray photoelectron spectroscopy (XPS). **d–f** Reproduced with permission from ref. [37] (copyright American Chemical Society, ACS 2022).

lattice distortion[46–48]. Similarly, entropy stabilization can also be achieved through mixing in the X sites, leading to bulk single-phase materials forming, as shown in Fig. 1d[49,50].

Various characterization methods are required to confirm the high configurational entropy of the system. X-ray/neutron diffraction[51], and scanning transmission electron microscopy combined with energy-dispersive X-ray spectroscopy, and high-angle annular dark-field methods have been used to delineate and map the principal elements[52]. Atomic scale tomographic techniques may also be explored to accentuate these methods[53,54]. Altering the stoichiometric ratio beyond the equimolar ratio can be used as a qualitative method to evaluate the effect of entropy in stabilizing the structure[34]. In addition, spectroscopy methods, such as X-ray photoelectron spectroscopy, are currently being implemented to understand the complex oxidation states and their effect on properties in high-entropy nanomaterials[55].

The elements and their coordination states affect these materials' interaction with surrounding species in the lattice. The compatibility of transition metals and post-transition metals in different coordination states can be examined to understand the role of charge transfer between the cations in a high-entropy material structure. In Fig. 2a, the compatibility of multi-valent metals in a cubic rock-salt lattice is demonstrated with their compatibility factor, labeled as the normalized temperature of mixing, or $T_{mix,\ normalized}$[56]. The compatibility, in this case, measures the propensity of a metal to transfer charge from one metal to another and maintain stability in a singular lattice. The green color, such as Fe^{3+} or V^{3+} with a $T_{mix,\ normalized} = 0.0$, is considered more compatible than the red elements, such as Zn^{2+} or Al^{3+} with a $T_{mix,\ normalized} = 1.0$[56]. In high-entropy materials, this charge transfer between the mixed metals plays a significant role in their inherent structural and electronic characteristics and their subsequent material properties.

2D high-entropy structures

The charge transfer process and changing local coordination states of metals within a high-entropy structure to create stable disordered lattice structures also impact the local strain within a lattice. The occupancy of multiple metal or non-metal sites in a 2D high-entropy material results in localized tensile and compressive strains on the lattice structure[57]. This strain results from the mixed atomic sizes of multi-valent distinct elements, as shown in Fig. 2b.

Using scanning transmission electron microscopy, the effect of five transition metals on the lattice can be seen by viewing the 2D structure perpendicular to the basal plane. By measuring the average distortion of the hexagonal lattice structure, the strain (red for tensile, blue for compressive) can be mapped onto the basal plane as seen in Fig. 1c for $(TiVZrNbTa)_2CT_x$ MXene[38], which demonstrates the local distortion caused by elements with various atomic radii in a single 2D material.

At the 2D nanosheet level, since most of the atoms are either on the surface or at the neighboring sites to the basal plane, localized strain and changes in electronic structure will have dominant effects on the material's properties. In a study on high-entropy 2D phosphorous trichalcogenides, $Co_x(VMnNiZn)_{1-x}PS_3$, the strain in the structure and localized changes in the electronic structure with their relative effects on the material's electrocatalysis behavior were explored[37]. A five-fold increase in the lattice strain was reported using powder X-ray diffraction on the bulk-layered phosphorous trichalcogenides. The high-entropy mixtures of $Co_x(VMnNiZn)_{1-x}PS_3$ also altered the X–X bond length (P–P bond here), and an increment-decrement relationship between the cobalt content and P–P bond length was observed (Fig. 2d). The effect of this P–P bond length change based on Co composition can be seen in Fig. 2e, where the highest hydrogen evolution reactivity is around a Co molar ratio of ~0.5. Because of these tunable P–P bonds, the authors speculate that a high-entropy structure could redistribute the electron density at each P atom and make it more active for electrocatalysis reactions. The authors also conducted X-ray photoelectron spectroscopy on $Co_{0.6}(VMnNiZn)_{0.4}PS_3$ and compared it with the corresponding single-metal phosphorous trichalcogenides ($CoPS_3$, VPS_3, $MnPS_3$, $NiPS_3$, and $ZnPS_3$). The results indicated the lowest binding energy states for both P and S, confirming a higher electron-donating character for the $[P_2S_6]^{4-}$ sites, which leads to better hydrogen adsorption in hydrogen evolution reactions (HER)[37]. The changes in the HER activity of $Co_x(VMnNiZn)_{1-x}PS_3$[37] demonstrate the effects of multiple elements on the electronic structure localized changes around cation and anion sites which can further control potential binding sites for energy storage or catalytic activity. However, further studies are necessary to fully investigate the effect of high entropy on the energy storage and conversion behavior of these 2D materials.

2D high-entropy materials in energy storage and conversion

There has been a growing research focus using the concept of high entropy in all components of an energy storage device, the electrodes (anode and cathode)[46,58], as well as solid-[59,60], and liquid-state electrolytes[61] (Fig. 3a, b). The possibility of tuning the bond length, electronic structure, and charge transfer in high-entropy materials coupled with the high surface area of 2D materials makes high-entropy 2D materials attractive candidates for energy storage and conversion. Current studies in high-entropy 2D systems have focused primarily on electrode materials.

The MXenes family has been explored extensively as electrode materials with research on their various synthesis techniques and modification strategies over the past decade[62,63]. However, it was not until recently that the high-entropy MXenes with four or more transition metal elements were reported[34,36,64]. These high-entropy MXenes are derived from their bulk precursors: the high-entropy MAX phases. While solid-solution double transition metal MAX phases have been studied for several decades, phase pure high-entropy MAX phases were not explored or reported independently of their 2D MXene counterparts.

As an outcome of the top-down synthesis approach, the MXenes' basal planes are decorated with functional moieties (such as –OH, = O, –F, –Cl, –S) bonded to the surface transition metal. The termination compositions depend highly on the synthesis route, providing another degree of tunability aside from the principal M and X elements[65]. The surface functional groups further control the electronic properties (metallic conductors to semiconductors, and superconductivity)[66,67], and stability.

So far, five compositions of high-entropy MXenes have been reported since 2021, and a few of them are being studied in energy storage applications. Those include $Ti_{1.1}V_{0.7}Cr_xNb_{1.0}Ta_{0.6}CT_x$ used as Li-ion battery (LIB) anode, Zn-ion[64], and H_2SO_4 supercapacitor electrodes[36], $(TiZrNbTa)_2CT_x$ and $(Ti_{0.2}V_{0.2}Zr_{0.2}Nb_{0.2}Ta_{0.2})_2C$ as LIB anodes[38], and $(TiVZrNbTa)_2CN$ as lithium–sulfur battery cathode[68]. When used as a LIB anode, delaminated $Ti_{1.1}V_{0.7}Cr_xNb_{1.0}Ta_{0.6}C_3T_x$ MXene film exhibited a first-cycle capacity of 126 mAh g^{-1} at 0.01 A g^{-1}, and a long-term stable capacitance of 40 mAh g^{-1} at 1 A g^{-1} for over 1000 cycles[64]. Although the charge storage capacities of high-entropy MXene are lower than (regular) $Ti_3C_2T_x$ MXene (410 mAh g^{-1} at 1 °C)[69], the high-entropy MXene exhibits an interesting cycle stability behavior: the steady-state capacity for high-entropy MXene increases two-fold after 300 cycles. This is while it decreases almost two-fold for $Ti_3C_2T_x$ MXene. When used as electrodes for Zn-ion[64] and H_2SO_4 electrolyte supercapacitors[36], a ~90% capacitance retention was seen after ~10,000 cycles. This demonstrates the increased cyclical stability of the system due to the implementation of a high-entropy 2D electrode.

The charge storage capacity of 2D materials, such as LIB electrodes, is generally limited by the extent of Li intercalation into the available space between the layers[70]. Consequently, simply by employing a high-entropy 2D electrode, the charge storage capacities will not necessarily be improved, and a more systematic design is required for high-entropy 2D electrodes. For example, Du et al.[68] showed how a high-entropy carbonitride MXene could capitalize on the ultra-high theoretical capacity of sulfur (1672 mAh g^{-1})[71] besides intercalation[72]. Benefiting from the high affinity and catalytic activity between the five different M–C/N bonds and polysulfides and the high mechanical strains in their carbonitride MXene layers, multistep sulfur conversion processes were shown to take place without the loss of active material. This has resulted in higher capacities (~900 mAh g^{-1} at 1 °C) and rate capabilities (702 mAh g^{-1} at 4 °C) with good cycling stability. Figure 3c summarizes the performance metrics of MXenes and layered transition metal oxides as models of high-entropy 2D materials used as battery electrodes in half-cell configurations.

The concept of high entropy in energy conversion has recently been introduced in other 2D materials, such as high-entropy transition metal chalcogenides. Wang et al. have recently reported >15-fold enhanced catalytic activity of $Co_{0.6}(VMnNiZn)_{0.4}PS_3$ toward HER compared to that of $CoPS_3$[37]. Owing to the composition-dependent electrocatalytic activities of the latter high-entropy material, it was found that by varying the Co content relative to other components, the following favorable properties are achieved: the material could be arbitrarily shifted left or right on the volcano plot[73]. This results in the highest population of active P and S sites for water dissociation and hydrogen adsorption with enhanced kinetics while minimizing the desorption energy barrier for adsorbed hydrogen intermediates to ensure a bond breakage and release of gaseous hydrogen (Fig. 3d). A similar mechanistic study has been reported earlier for ammonia decomposition using a series of bulk $Co_xMo_yFeNiCu$ ($x + y = 7$) nanoparticles (non-2D) by tuning the Co/Mo ratios[74].

Given the earth-abundant non-precious elements employed in the fabrication of 2D-electrocatalysts and the high level of compositional tunability, their application in (non-2D) catalysis is an emerging field of research[75–78]. In the 2D space, a recent study synthesized and used a high-entropy 2D transition metal dichalcogenide $(MoWVNbTa)S_2$ for electrocatalytic CO_2 capture

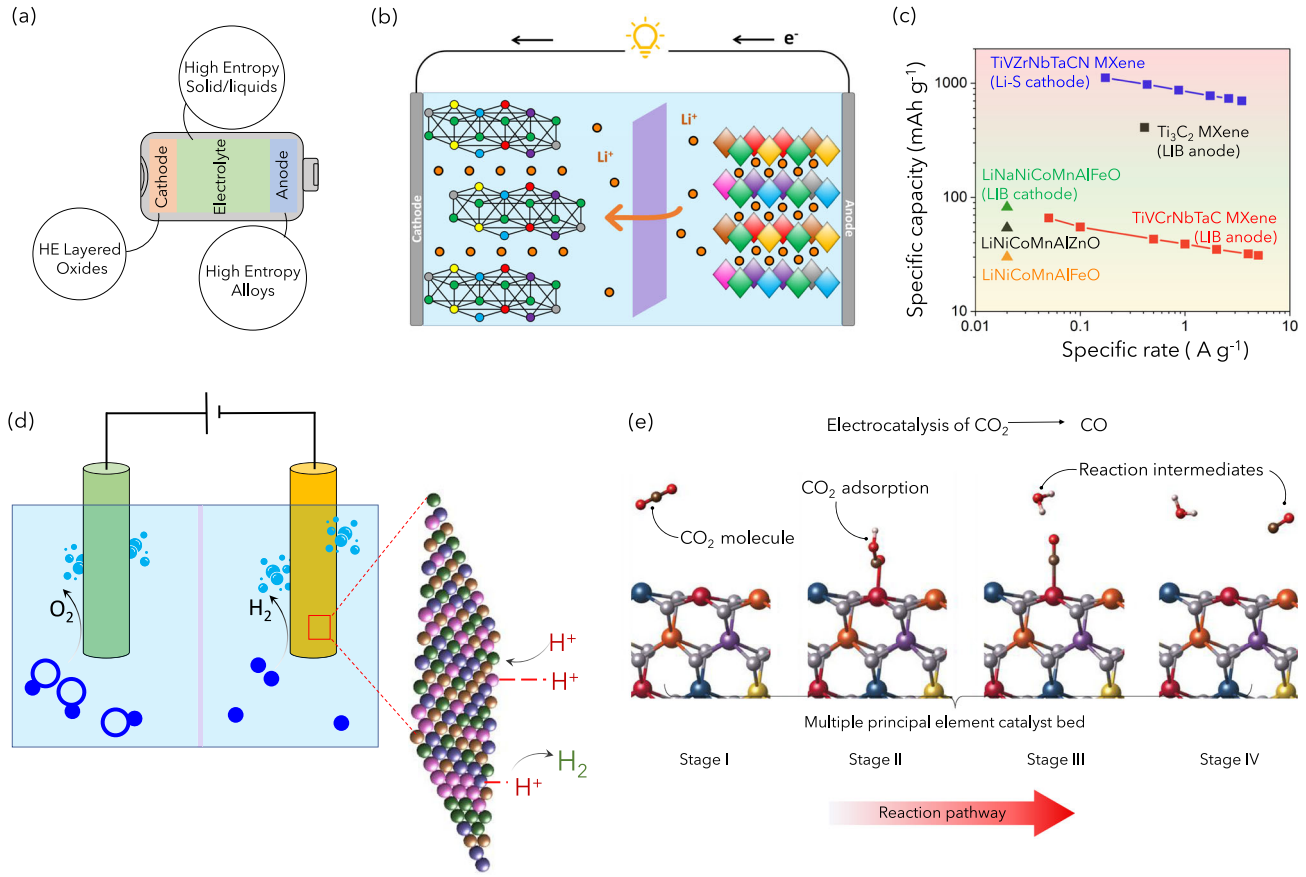

Fig. 3 High-entropy 2D materials for energy storage and conversion. Schematic representation of **a** a 'high-entropy battery' where anode, cathode, and electrolyte are all made of high-entropy materials; **b** Li-ion batteries composed of a high-entropy 2D intercalation material (such as MXene) and a 3D conversion material (oxides/sulfides) with improved cycle-stability owing to their high configurational entropy; **c** summary of capacities and rate handling capabilities of different high-entropy materials, marked by color codes denoting how recent each material was introduced to the community; **d** high-entropy 2D electrocatalysts used for hydrogen and oxygen evolution reactions, magnifying microscopic interactions of protons with different elements from the surface of the high-entropy electrode and their ultimate conversion into hydrogen molecule. **d** Adapted with permission from ref. [74] (copyright Springer Nature, 2019); **e** electrocatalysis reaction steps of CO_2 conversion into CO at a transition metal site of a (Mo, W, V, Nb, Ta)S_2 nanoribbon. **e** Reproduced with permission from ref. [42] (copyright Wiley, 2021).

and its conversion into CO[42]. Aided by computational studies, this high-entropy 2D material with equimolar transition metal composition is first screened and verified regarding miscibility, enthalpic and entropic stabilities and then synthesized and tested for electrochemical performance. Figure 3e schematically shows the stepwise process (from I to IV) of the CO_2 reduction reaction at a transition metal site in (MoWVNbTa)S_2[42]. The following steps are hypothesized based on the simulation and experiments: (I and II) as a CO_2 molecule approaches the surface, it adsorbs on the transition metal with strong binding affinity, resulting in the formation of COOH* and CO* reaction intermediates; (III and IV) the reduced desorption energy barrier caused by the disordered (because of the high-entropy system) and neighboring coordinated metal atoms facilitate the bond breakage of the product (CO)[76,79]. There is also the possibility of CO* hopping from stronger binding elements (W and Mo) to weaker binding elements (for example, vanadium).

Outlook

Fundamentally, many questions are yet to be answered in this new field of high-entropy 2D materials. Mechanisms that explain the stability and performance of bulk high-entropy materials can aid in providing insights. For example, the cocktail effect, which is prominent in bulk materials and contributes significantly toward property enhancement, may not be dominant in a 2D system as demonstrated in high-entropy MXenes, which have been computationally predicted to exhibit some short-range order of atoms in different atomic planes[37], which still requires experimental verifications. In addition, those 2D systems synthesized via top-down approaches have the presence of surface terminal groups which can affect the electronic structure of the surface or edge-site metallic species[80].

Another challenge is to identify stable compositions tailored to specific applications. One approach to mitigate instability can be introducing disorder in the non-metal sub-lattices, as a substitutional disorder in these sites will increase the entropy of mixing. For example, adding fluoride salts to high-entropy oxides led to greater stabilities and higher working potentials (3.4 V vs. Li^+/Li) for cathode materials[81]. Similar mixing, in principle, is adaptable to other systems such as 2D chalcogenides. Mixing in non-metal such as in 2D transition metal borocarbonitrides ($B_xC_yN_z$) with B, C, and N, all forming an alloy in the non-metallic sublattice can be functionalized toward efficient hydrogen storage and carbon sequestering[82]. A potential avenue for high-entropy 2D materials is envisioned for selective ion-sieving and sensing applications. Specifically, with tailorable basal atomic plane activity, the effects of fermi energy and spillover phenomena observed in high-entropy alloys can be better understood at the nanoscale to develop highly efficient sensing devices[83]. The

high-entropy 2D compounds can provide a platform to understand better the correlation of electronic structure and the improvement of mechanical properties reported in some bulk high-entropy carbides[84].

Studies on composition–structure–property relationships in 2D high-entropy systems are at a nascent stage. Models such as entropy descriptors[20], valence electron concentration[85] atomic radii, and electronegativity can be adapted for identifying stable compositions. In addition, using paired experimental and computational approaches can assist in the characterization and understanding of localized interactions. However, more development is necessary to handle the increased computational complexity due to these structures' size and facet dependency[86]. Yet, considering an immense number of possible 2D high-entropy compositions, modeling and predictive material science (in combination with high-throughput surveying) will play critical roles in advancing the research field[87].

Future development of high entropy principles at the nanoscale will be the most direct pairing of 2D materials' unique electronic structure with the high surface area toward energy storage, catalytic activity, magnetic behavior, mechanical properties, and other applications. As continued development of these materials moves into the current decade and beyond, we believe that high-entropy 2D materials will provide a wide degree of tunability and control, unlike other composition–structure–property techniques in materials science for the fundamental study of the high-entropy concept and address energy, catalytic, electronic, and structural challenges of our world.

Received: 16 December 2022; Accepted: 2 February 2023;
Published online: 21 February 2023

References

1. Zolotukhin, I. V. & Kalinin, Y. E. Amorphous metallic alloys. *Sov. Phys. Usp.* **33**, 720 (1990).
2. Eylon, D., Fujishiro, S., Postans, P. J. & Froes, F. H. High-temperature titanium alloys—a review. *JOM* **36**, 55–62 (1984).
3. Murty, B. S., Yeh, J. W., Ranganathan, S. & Bhattacharjee, P. P. A brief history of alloys and the birth of high-entropy alloys. In *High-Entropy Alloys* 2nd edn (eds Murty, B. S., Yeh, J. W., Ranganathan, S. & Bhattacharjee, P. P.) (Elsevier, 2019).
4. George, E. P., Raabe, D. & Ritchie, R. O. High-entropy alloys. *Nat. Rev. Mater.* **4**, 515–534 (2019).
5. Cantor, B., Chang, I. T. H., Knight, P. & Vincent, A. J. B. Microstructural development in equiatomic multicomponent alloys. *Mater. Sci. Eng.: A* **375–377**, 213–218 (2004). **Seminal work on high-entropy alloys**.
6. Gao, M. C., Yeh, J.-W., Liaw, P. K. & Zhang, Y. *High-entropy Alloys*. (Springer International Publishing, Cham, 2016).
7. Yeh, J. W. et al. Nanostructured high-entropy alloys with multiple principal elements: novel alloy design concepts and outcomes. *Adv. Eng. Mater.* **6**, 299–303 (2004). **Among the first reports on high-entropy alloys**.
8. Miracle, D. High entropy alloys as a bold step forward in alloy development. *Nat. Commun.* **10**, 1–3 (2019).
9. Li, J., Fang, Q. & Liaw, P. K. Microstructures and properties of high-entropy materials: modeling, simulation, and experiments. *Adv. Eng. Mater.* **23**, 2001044 (2021).
10. Lei, Z. et al. Enhanced strength and ductility in a high-entropy alloy via ordered oxygen complexes. *Nature* **563**, 546–550 (2018).
11. Huang, T. et al. Effect of carbon addition on the microstructure and mechanical properties of CoCrFeNi high entropy alloy. *Sci. China Technol. Sci.* **61**, 117–123 (2018).
12. Wu, M., Li, Z., Gault, B., Munroe, P. & Baker, I. The effects of carbon on the phase stability and mechanical properties of heat-treated FeNiMnCrAl high entropy alloys. *Mater. Sci. Eng. A* **748**, 59–73 (2019).
13. Luo, H. et al. Beating hydrogen with its own weapon: nano-twin gradients enhance embrittlement resistance of a high-entropy alloy. *Mater. Today* **21**, 1003–1009 (2018).
14. Chen, T. K., Shun, T. T., Yeh, J. W. & Wong, M. S. Nanostructured nitride films of multi-element high-entropy alloys by reactive DC sputtering. *Surf. Coat. Technol.* **188-189**, 193–200 (2004).
15. Moskovskikh, D. et al. Extremely hard and tough high entropy nitride ceramics. *Sci. Rep.* **10**, 19874 (2020).
16. Sarkar, A. et al. High entropy oxides for reversible energy storage. *Nat. Commun.* **9**, 3400 (2018).
17. Rost, C. M. et al. Entropy-stabilized oxides. *Nat. Commun.* **6**, 1–8 (2015). **Among the first reports on high-entropy oxide ceramics**.
18. Gild, J. et al. High-entropy fluorite oxides. *J. Eur. Ceram. Soc.* **38**, 3578–3584 (2018).
19. Zhang, J. et al. High-entropy oxides $10La_2O_3-20TiO_2-10Nb_2O_5-20WO_3-20ZrO_2$ amorphous spheres prepared by containerless solidification. *Mater. Lett.* **244**, 167–170 (2019).
20. Sarker, P. et al. High-entropy high-hardness metal carbides discovered by entropy descriptors. *Nat. Commun.* **9**, 4980 (2018).
21. Castle, E., Csanádi, T., Grasso, S., Dusza, J. & Reece, M. Processing and properties of high-entropy ultra-high temperature carbides. *Sci. Rep.* **8**, 1–12 (2018).
22. Gild, J. et al. High-entropy metal diborides: a new class of high-entropy materials and a new type of ultrahigh temperature ceramics. *Sci. Rep.* **6**, 37946 (2016).
23. Gild, J. et al. A high-entropy silicide: $(Mo_{0.2}Nb_{0.2}Ta_{0.2}Ti_{0.2}W_{0.2})Si_2$. *J. Materiom.* **5**, 337–343 (2019).
24. Qin, Y. et al. A high entropy silicide by reactive spark plasma sintering. *J. Adv. Ceram.* **8**, 148–152 (2019).
25. Jiang, B. et al. High-entropy-stabilized chalcogenides with high thermoelectric performance. *Science* **371**, 830–834 (2021).
26. Yang, J. X. et al. Rapid fabrication of high-entropy ceramic nanomaterials for catalytic reactions. *ACS Nano* **15**, 12324–12333 (2021).
27. Ding, S. et al. Plasma-regulated two-dimensional high entropy oxide arrays for synergistic hydrogen evolution: from theoretical prediction to electrocatalytic applications. *J Power Sources* **520**, 230873 (2022).
28. Dudnik, O. V. et al. High-entropy ceramics for thermal barrier coatings produced from ZrO_2 doped with rare-earth metal oxides. *Powder Metall. Metal Ceram.* **59**, 556–563 (2021).
29. Li, F., Zhou, L., Liu, J.-X., Liang, Y. & Zhang, G.-J. High-entropy pyrochlores with low thermal conductivity for thermal barrier coating materials. *J. Adv. Ceram.* **8**, 576–582 (2019).
30. Zhai, S. et al. The use of poly-cation oxides to lower the temperature of two-step thermochemical water splitting. *Energy Environ. Sci.* **11**, 2172–2178 (2018).
31. Wright, A. J. & Luo, J. A step forward from high-entropy ceramics to compositionally complex ceramics: a new perspective. *J. Mater. Sci.* **55**, 9812–9827 (2020).
32. Niu, B. et al. Sol–gel autocombustion synthesis of nanocrystalline high-entropy alloys. *Sci. Rep.* **7**, 3421 (2017). **Amongst the first reports on nanocrystalline high-entropy alloys**.
33. Miura, A., Ishiyama, S., Kubo, D., Rosero-Navarro, N. C., & Tadanaga, K. Synthesis and ionic conductivity of a high-entropy layered hydroxide. *J. Ceram. Soc. Jpn.* **128**, 336–339 (2020).
34. Nemani, S. K. et al. High-entropy 2D carbide MXenes: $TiVNbMoC_3$ and $TiVCrMoC_3$. *ACS Nano* **15**, 12815–12825 (2021). **Among the first papers on high-entropy 2D MXenes and the first on $M_4C_3T_x$ MXenes**.
35. Li, F. et al. Bottom-up synthesis of 2D layered high-entropy transition metal hydroxides. *Nanoscale Adv.* **4**, 2468–2478 (2022). **Among the first papers on high-entropy 2D transition metal hydroxides**.
36. Zhou, J. et al. High-entropy laminate metal carbide (MAX Phase) and its two-dimensional derivative MXene. *Chem. Mater.* **34**, 2098–2106 (2022).
37. Wang, R. et al. Two-dimensional high-entropy metal phosphorus trichalcogenides for enhanced hydrogen evolution reaction. *ACS Nano* **16**, 3593–3603 (2022).
38. Du, Z. et al. High-entropy atomic layers of transition-metal carbides (MXenes). *Adv. Mater.* **33**, 2101473 (2021). **Among the first papers on high-entropy 2D MXenes and the first on an M_2CT_x high-entropy MXene**.
39. Cui, Y. et al. A perspective on high-entropy two-dimensional materials. *SusMat* **2**, 65–75 (2022).
40. Wu, L. et al. Electrocatalysts toward oxygen evolution reaction. *Adv. Funct. Mater.* **33**, 2208170 (2023).
41. Teplonogova, M. A., Yapryntsev, A. D., Baranchikov, A. E. & Ivanov, V. K. High-entropy layered rare earth hydroxides. *Inorg. Chem.* **61**, 19817–19827 (2022).
42. Cavin, J. et al. 2D High-entropy transition metal dichalcogenides for carbon dioxide electrocatalysis. *Adv. Mater.* **33**, 2100347 (2021). **Among the first reports on high-entropy 2D transition metal dichalogenides**.
43. Ying, T. et al. High-entropy van der Waals materials formed from mixed metal dichalcogenides, halides, and phosphorus trisulfides. *J. Am. Chem. Soc.* **143**, 7042–7049 (2021).
44. Rao, Z. et al. Beyond solid solution high-entropy alloys: tailoring magnetic properties via spinodal decomposition. *Adv. Funct. Mater.* **31**, 2007668 (2021).
45. Wu, Y. et al. Short-range ordering and its effects on mechanical properties of high-entropy alloys. *J. Mater. Sci. Technol.* **62**, 214–220 (2021).

46. Oses, C., Toher, C. & Curtarolo, S. High-entropy ceramics. *Nat. Rev. Mater.* **5**, 295–309 (2020).
47. Rost, C. M., Rak, Z., Brenner, D. W. & Maria, J. P. Local structure of the $Mg_xNi_xCo_xCu_xZn_xO$ ($X = 0.2$) entropy-stabilized oxide: an EXAFS study. *J. Am. Ceram. Soc.* **100**, 2732–2738 (2017).
48. Berardan, D., Meena, A., Franger, S., Herrero, C. & Dragoe, N. Controlled Jahn–Teller distortion in (MgCoNiCuZn) O-based high entropy oxides. *J. Alloys Compd.* **704**, 693–700 (2017).
49. Li, F. et al. Synthesis of single-phase metal oxycarbonitride ceramics. *Scr. Mater.* **176**, 17–22 (2020).
50. Wen, T., Liu, H., Ye, B., Liu, D. & Chu, Y. High-entropy alumino-silicides: a novel class of high-entropy ceramics. *Sci. China Mater.* **63**, 300–306 (2020).
51. Wang, F. et al. The effect of submicron grain size on thermal stability and mechanical properties of high-entropy carbide ceramics. *J. Am. Ceram. Soc.* **103**, 4463–4472 (2020).
52. Dusza, J. et al. Microstructure of (Hf–Ta–Zr–Nb)C high-entropy carbide at micro and nano/atomic level. *J. Eur. Ceram. Soc.* **38**, 4303–4307 (2018).
53. Hu, R., Jin, S. & Sha, G. Application of atom probe tomography in understanding high entropy alloys: 3D local chemical compositions in atomic scale analysis. *Prog. Mater. Sci.* **123**, 100854 (2022).
54. Pradeep, K. G. et al. Atomic-scale compositional characterization of a nanocrystalline AlCrCuFeNiZn high-entropy alloy using atom probe tomography. *Acta Mater.* **61**, 4696–4706 (2013).
55. Wang, D. et al. Low-temperature synthesis of small-sized high-entropy oxides for water oxidation. *J. Mater. Chem. A* **7**, 24211–24216 (2019).
56. Lun, Z. et al. Cation-disordered rocksalt-type high-entropy cathodes for Li-ion batteries. *Nat. Mater.***20**, 214–221 (2021).
57. Hedman, D., Feltrin, A. C., Miyamoto, Y. & Akhtar, F. Ab-initio aided design of novel quaternary, quinary and senary high-entropy borocarbides. *J. Mater. Sci.* **57**, 422–443 (2022).
58. Fu, M., Ma, X., Zhao, K., Li, X. & Su, D. High-entropy materials for energy-related applications. *Iscience* **24**, 102177 (2021).
59. Wu, B. et al. High-entropy NASICON phosphates (Na_3M_2 $(PO_4)_3$ and $NaMPO_4O_x$, M = Ti, V, Mn, Cr, and Zr) for sodium electrochemistry. *Inorg. Chem.* **61**, 4092–4101 (2022).
60. Guo, R. & He, T. High-entropy Perovskite electrolyte for protonic ceramic fuel cells operating below 600 °C. *ACS Mater. Lett.* **4**, 1646–1652 (2022).
61. Zhang, W. et al. Decimal solvent-based high-entropy electrolyte enabling the extended survival temperature of lithium-ion batteries to −130 °C. *CCS Chem.* **3**, 1245–1255 (2021).
62. Gogotsi, Y. & Anasori, B. The rise of MXenes. *ACS Nano* **13**, 8491–8494 (2019).
63. Anasori, B. & Gogotsi, Y. MXenes: trends, growth, and future directions. *Graphene 2D Mater.* **7**, 75–79 (2022).
64. Etman, A. S., Zhou, J. & Rosen, J. $Ti_{1.1}V_{0.7}Cr_xNb_{1.0}Ta_{0.6}C_3T_z$ high-entropy MXene freestanding films for charge storage applications. *Electrochem. Commun.* **137**, 107264 (2022).
65. Lim, K. R. G. et al. Fundamentals of MXene synthesis. *Nat. Synth.* **1**, 601–614 (2022).
66. Li, X. et al. MXene chemistry, electrochemistry and energy storage applications. *Nat. Rev. Chem.* **6**, 1–16 (2022).
67. Kamysbayev, V. et al. Covalent surface modifications and superconductivity of two-dimensional metal carbide MXenes. *Science* **369**, 979–983 (2020).
68. Du, Z. et al. High-entropy carbonitride MAX phases and their derivative MXenes. *Adv. Energy Mater.* **12**, 2103228 (2022).
69. Mashtalir, O. et al. Intercalation and delamination of layered carbides and carbonitrides. *Nat. Commun.* **4**, 1716 (2013).
70. Kanno R. Secondary batteries—lithium rechargable systems | electrolytes: solid sulfide. In *Encyclopedia of Electrochemical Power Sources* (ed Garche, J.) (Elsevier, 2009).
71. Kim, J. H. et al. Encapsulation of S/SWNT with PANI Web for enhanced rate and cycle performance in lithium sulfur batteries. *Sci. Rep.* **5**, 8946 (2015).
72. Zhao, T. et al. Electrochemical lithiation mechanism of two-dimensional transition-metal dichalcogenide anode materials: intercalation versus conversion reactions. *J. Phys. Chem. C* **123**, 2139–2146 (2019).
73. Kakaei, K., Esrafili, M. D., & Ehsani, A. Alcohol oxidation and hydrogen evolution. In *Interface Science and Technology* (eds Kakaei, K., Esrafili, M. D., & Ehsani, A.) (Elsevier, 2019).
74. Xie, P. et al. Highly efficient decomposition of ammonia using high-entropy alloy catalysts. *Nat. Commun.* **10**, 4011 (2019).
75. Sun, Y. & Dai, S. High-entropy materials for catalysis: a new frontier. *Sci. Adv.* **7**, 1600 (2021).
76. Batchelor, T. A. A. et al. High-entropy alloys as a discovery platform for electrocatalysis. *Joule* **3**, 834–845 (2019).
77. Yu, L. et al. High-entropy alloy catalysts: from bulk to nano toward highly efficient carbon and nitrogen catalysis. *Carbon Energy* **4**, 731–761 (2022).
78. Sun, Y. et al. Battery-driven N_2 electrolysis enabled by high-entropy catalysts: from theoretical prediction to prototype model. *Small* **18**, 2106358 (2022).
79. Wang, S. & Xin, H. Predicting catalytic activity of high-entropy alloys for electrocatalysis. *Chem* **5**, 502–504 (2019).
80. Xie, Y. et al. Role of surface structure on Li-ion energy storage capacity of two-dimensional transition-metal carbides. *J. Am. Chem. Soc.* **136**, 6385–6394 (2014).
81. Wang, Q. et al. Multi-anionic and-cationic compounds: new high entropy materials for advanced Li-ion batteries. *Energy Environ. Sci.* **12**, 2433–2442 (2019).
82. Muraleedharan, M. G. & Kent, P. R. C. Novel boron nitride MXenes as promising energy storage materials. *Nanoscale* **14**, 9086–9096 (2022).
83. Schweizer-Berberich, M. et al. The effect of Pt and Pd surface doping on the response of nanocrystalline tin dioxide gas sensors to CO. *Sensors Actuators B Chem.* **31**, 71–75 (1996).
84. Harrington, T. J. et al. Phase stability and mechanical properties of novel high entropy transition metal carbides. *Acta Mater.* **166**, 271–280 (2019).
85. Zhang, R.-Z., Gucci, F., Zhu, H., Chen, K. & Reece, M. J. Data-driven design of ecofriendly thermoelectric high-entropy sulfides. *Inorg. Chem.* **57**, 13027–13033 (2018).
86. Löffler, T. et al. Toward a paradigm shift in electrocatalysis using complex solid solution nanoparticles. *ACS Energy Lett.* **4**, 1206–1214 (2019).
87. Wang, Q., Velasco, L., Breitung, B. & Presser, V. High-entropy energy materials in the age of big data: a critical guide to next-generation synthesis and applications. *Adv. Energy Mater.* **11**, 2102355 (2021).
88. Liu, R. et al. Entropy as a gene-like performance indicator promoting thermoelectric materials. *Adv. Mater.* **29**, 1702712 (2017).

Acknowledgements

The INM authors acknowledge funding of the MXene-CDI project (PR-1173/11) by the German Research Foundation (DFG, Deutsche Forschungsgemeinschaft). S.K.N., B.C.W., and B.A. thank the US Office of Naval Research (ONR) under award number N00014-21-1-2799 and US National Science Foundation under grant number 2124478.

Author contributions

S.K.N., M.T., and B.C.W. conducted the literature search and prepared the first draft of the paper and the figures. V.P. proposed the idea. V.P. and B.A. supervised, reviewed, edited the paper, and acquired the funding. All authors revised and discussed the final manuscript.

Competing interests

The authors declare no competing interests.

Additional information

Supplementary information The online version contains supplementary material available at https://doi.org/10.1038/s43246-023-00341-y.

Correspondence and requests for materials should be addressed to Volker Presser or Babak Anasori.

Peer review information *Communications Materials* thanks the anonymous reviewers for their contribution to the peer review of this work. Primary Handling Editor: John Plummer. Peer reviewer reports are available.